Fabrication and Characterization of GaN/Polymer Composite *p–n* Junction with PEDOT Nanoparticle Interface Layer

M.S. Kim[a], S.-M. Jin[b], H.Y. Choi[a], G.S. Kim[a], K.G. Yim[a], S. Kim[c], G. Nam[c], H.S. Yoon[c], Y. Kim[a], D.-Y. Lee[d], Jin S. Kim[c], Jong S. Kim[f] and J.-Y. Leem[a,b,*]

[a]Department of Nano Systems Engineering, Center for Nano Manufacturing, Inje University Gimhae 621-749, Republic of Korea

[b]Ink Technology Center, Ink Tec. Co. Ltd., Pyeongtaek 451-821, Republic of Korea

[c]School of Nano Engineering, Inje University, Gimhae 621-749, Republic of Korea

[d]Epi-manufacturing Technology, Samsung LED Co., Ltd., Suwon 443-373, Republic of Korea

[e]Division of Advanced Materials Engineering, Chonbuk National University, Jeonju 561-756, Republic of Korea

[f]Department of Physics, Yeungnam University, Gyeongsan 712-749, Republic of Korea

(Received December 23, 2010)

A heavily Si-doped GaN/polymer hybrid structure with *p*-type poly(3,4-ethylene-dioxythiophene):beta-1,3--glucan (PEDOT nanoparticle) interface layer has been fabricated. The Si-doped GaN thin film with carrier concentration of 1×10^{19} cm^{-3} was grown by metal-organic chemical vapor deposition. The PEDOT nanoparticle with various sizes ranging from 60 to 120 nm was synthesized via a miniemulsion polymerization process. The electrical conductivity of the PEDOT nanoparticle is less than 1.2 S/cm. The current–voltage (I–V) characteristic of the hybrid structure shows diode-like behavior. The I–V characteristic was examined in the framework of the thermionic emission model. The ideality factor of the structure without PEDOT nanoparticle interface layer is 12.9. However, the ideality factor of the hybrid structure with PEDOT nanoparticle interface layer is obtained as 1.9. The value of ideality factor is dramatically decreased by inserting the PEDOT nanoparticle interface layer.

PACS: 73.61.Ey, 81.15.Gh

1. Introduction

Gallium nitride (GaN) is a promising material for UV/blue light-emitting diodes and high power temperature devices. These electronic and optoelectronic devices included visible light-emitting diodes (LED) [1], metal semiconductor field effects transistors (MESFET) [2], high electron mobility transistors (HEMT) [3], UV photoconductive detectors [4], and UV photovoltaic detectors [5]. The fabrication of the devices requires performing a controlled and reproducible n- and p-type doping. Many works were done to study n-type doping of GaN. Silicon (Si), germanium (Ge), and selenium (Se) have been used as dopants [6, 7]. Satisfactory electrical properties of Si-doped GaN have been reported but still suffer from compensation effects [8]. Heavily doped materials with low electrical resistivity will lead to novel device and contact metallization designs for high power and high efficiency light emitters [9]. In most cases, the optoelectronic devices are fabricated by growing GaN thin films on top of different substrates, usually sapphire, Si, or SiC, using various growth methods [10, 11].

Hybrid structures consisting of inorganic components including low-dimensional system and organic components have recently attracted considerable attention due to the advantages of the organic and inorganic materials, such as modified light-matter interaction, low cost spin-coating process, and mechanical flexibility [12, 13]. Spin coating of organic components may result in better junction properties since physical and chemical stresses are much lower at the interface than with other process techniques [14]. Conducting polymers are an attractive class of materials that combine the general properties of traditional organic polymers with the electrical conductivity of metals or semiconductors. They have potential applications in electrochromics [15], supercapacitors [16], antistatic and electrostatic coatings [17], light-emitting devices [18], photovoltaics [19], and sensors [20]. However, their insolubility in some solvents limits their wider use.

Among conducting polymers, poly(3,4-ethylene-dioxythiophene) (PEDOT) has been well investigated due to its good environmental stability, low band gap, low redox potential, and high optical transparency in its electrically conductive state, all properties that make it an excellent candidate for use in optoelectronics [21, 22]. Despite the fact that the PEDOT:poly(styrenesulfonate) (PEDOT:PSS) mixture is largely used for photoelectronics, there is still a need to optimize the synthesis and the morphology of PEDOT in order to tune the optoelectronic properties. Many groups have reported different

* corresponding author; e-mail: jyleem@inje.ac.kr

techniques to synthesize PEDOT nanoobjects with the aim of improving its processability [23–25]. Recently, Sun and Hanger reported the synthesis of PEDOT nanowires in the presence of poly (acrylic acid) [26]. We also synthesized the p-type poly(3,4-ethylene-dioxythiophene):beta--1,3-glucan (PEDOT nanoparticle).

In this work, a hybrid structure comprised of heavily Si-doped GaN and PEDOT:PSS with PEDOT nanoparticle interface layer was fabricated. The field-emission scanning electron microscopy (FE-SEM), transmission electron microscopy (TEM), photoluminescence (PL), the Hall effect, and current–voltage (I–V) measurement were carried out to investigate the properties of the Si--doped GaN thin film, the PEDOT nanoparticle, and their hybrid structure.

2. Experimental details

2.1. Synthesis of PEDOT nanoparticle

The organic phase made up of 3,4-ethylene-dioxythiophene (EDOT) and a hydrophobe was thoroughly mixed with the aqueous phase including deionized (DI) water and surfactant. Then, the resulting mixture was transferred to an ultrasonifier and treated for 10 min in an ice bath. The chemical oxidative polymerization was initiated with the addition of the aqueous oxidant solution in the reaction mixture, and the reaction was maintained at 35 ℃ for 48 h in a nitrogen atmosphere. After the completion of polymerization, the solid products were recovered from the reaction mixture by filtration and cleaning with a copious amount of DI water. The precipitated particles were separated by thrice-repeated centrifugation and then dried under vacuum at 60 ℃ for 24 h.

2.2. Fabrication of the hybrid structure

Figure 1 shows the cross-section schematic diagram of the hybrid structure. The GaN thin film was grown on

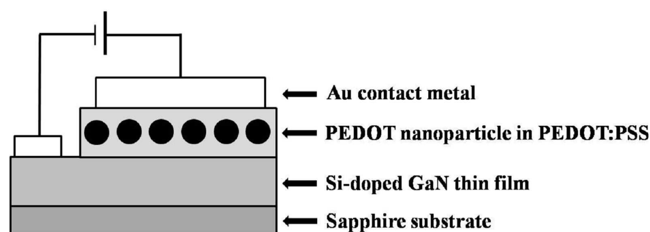

Fig. 1. Cross-section schematic diagram of the hybrid structure.

sapphire substrate by metal-organic chemical vapor deposition (MOCVD). Prior to the growth of GaN, the substrate was nitridated at high temperature under N_2 ambient. Then, the GaN nucleation layer was deposited at low temperature. The undoped GaN layer with the thickness of 1.5 μm and the Si-doped GaN layer with the thickness of 2 μm were grown at 1100 ℃. The PEDOT:PSS was deposited by spin-coating method with the rotation speed of 3000 rpm for 20 s, and then PEDOT nanoparticle was sprinkled. The PEDOT:PSS was again deposited onto PEDOT nanoparticle. A thin layer of gold (Au) was deposited on top of the polymer layer and the Si-doped GaN thin film.

3. Results and discussion

Figure 2 shows (a) FE-SEM and (b) TEM image of the PEDOT nanoparticle. The PEDOT nanoparticle for FE--SEM analysis was coated with Pt/Pd by sputtering for 150 s. The FE-SEM images were obtained on a Hitachi Model S-4300SE operating at 5 kV. Drops of aqueous PEDOT emulsion were dried on a carbon-coated copper grid for TEM analyst, and the TEM images were obtained on a Hitachi Model H-7500 operating at 80 kV. The morphology and size of the PEDOT particle are dependent on the operation conditions of the ultrasonifier treatment in the miniemulsion polymerization process. In this work, the PEDOT spherical nanoparticle with various size ranging from 60 to 120 nm was used.

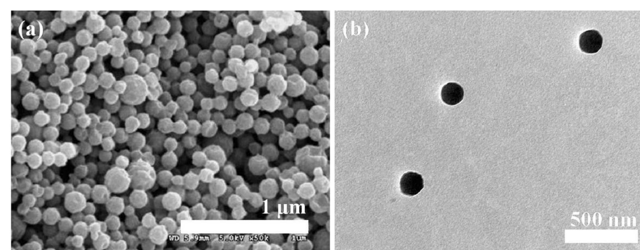

Fig. 2. (a) FE-SEM and (b) TEM image of the PEDOT nanoparticle.

The electrical conductivity was measured using a Mitsubishi Chemical Analytech Model Loresta-EP MCP--T360 four-probe resistivity meter at room temperature. For the preparation of electrical conductivity specimen, the vacuum-dried PEDOT nanoparticle was comingled with a small portion of carboxymethyl cellulose (CMC) (< 5 wt%) in the presence of DI water and then ground with pestle in a mortar. The rectangular-shaped thin specimen with a dimension of 7 mm $\times$ 7 mm was prepared by coating it with the PEDOT nanoparticle slurry using a doctor blade. The specimen was dried under vacuum at 60 ℃ for 24 h and then transferred for the electrical conductivity measurement. The electrical conductivity of the PEDOT nanoparticle is less than 1.2 S/cm due to the presence of β-1,3-glucan molecules along with PEDOT. The electrical conductivity was measured using a Mitsubishi Chemical Analytech Model Loresta-EP MCP--T360 four-probe resistivity meter at room temperature. For the preparation of electrical conductivity specimen, the vacuum-dried PEDOT nanoparticle was comingled with a small portion of carboxymethyl cellulose (CMC) (< 5 wt%) in the presence of DI water and then ground with pestle in a mortar. The rectangular-shaped thin specimen with a dimension of 7 mm $\times$ 7 mm was prepared

by coating it with the PEDOT nanoparticle slurry using a doctor blade. The specimen was dried under vacuum at 60 °C for 24 h and then transferred for the electrical conductivity measurement. The electrical conductivity of the PEDOT nanoparticle is less than 1.2 S/cm due to the presence of β-1,3-glucan molecules along with PEDOT.

The room temperature PL spectrum of the Si-doped GaN thin film by using a He–Cd laser with an excitation power of 30 mW and a 1 m single-grating monochromator with a photomultiplier tube is shown in Fig. 3. A weak peak at 365 nm with full width at half maximum (FWHM) of 5.6 nm and a strong broad peak at 560 nm with FWHM of 106 nm are observed. The peak at 365 nm in the ultraviolet (UV) emission region is related to near-band-edge emission. It originates from the recombination of excitons near the band-edge. The strong yellow emission peak corresponding to 560 nm is related to defects [27]. The obvious Fabry–Perot interference from the PL spectrum is observed due to a mirror-like thin film of GaN on sapphire substrate [28]. The carrier concentration in the Si-doped GaN thin film is 1×10^{-19} cm^{-3} obtained from the Hall effect measurement with the Van der Pauw method.

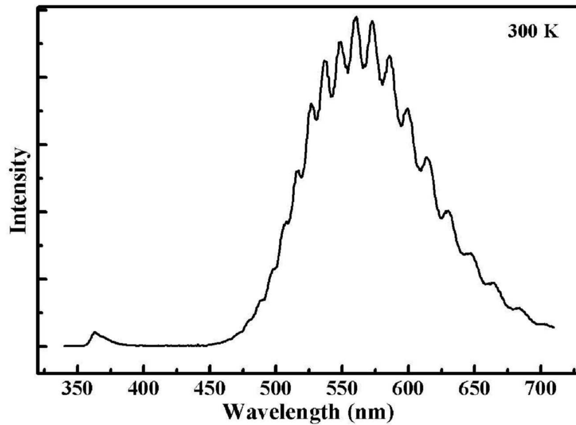

Fig. 3. PL spectrum of the heavily Si-doped GaN thin film.

Figure 4 shows 30° tilt FE-SEM image of the PEDOT nanoparticle embedded in the polymer layer of the hybrid structure. The density of the PEDOT nanoparticle is about 3.5×10^{10} cm^{-2}.

Figure 5 shows I–V characteristics of the PEDOT:PSS/Si-doped GaN and the hybrid structure. A positive voltage was applied to the polymer layer and a negative voltage was applied to the Si-doped GaN thin film. The I–V characteristic shows diode-like behavior. The threshold voltage of the hybrid structure compared with the PEDOT:PSS/GaN structure with almost the same thickness of polymer layer was increased. The increase in the threshold voltage suggests that there is a higher barrier for charge injection from electrodes into the Si-doped GaN thin film. For further investigation, I–V curve of the Si-doped GaN (without polymer layer)

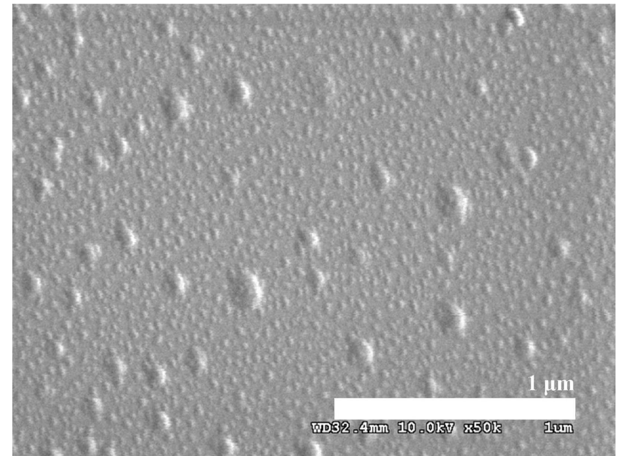

Fig. 4. 30° tilt FE-SEM image of the PEDOT nanoparticle embedded in the polymer layer of the hybrid structure.

was fabricated, which exhibits only a conductor behavior, indicating that the PEDOT:PSS forms lower energy barrier as composed with the heavily Si-doped GaN thin film. The energy barrier height of the hybrid structure is more increased by the PEDOT nanoparticle interface layer.

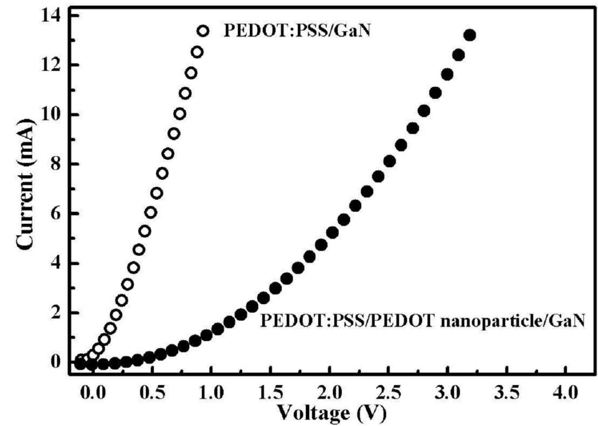

Fig. 5. Current–voltage (I–V) characteristics of the PEDOT:PSS/Si-doped GaN and the hybrid structure.

The diode-like behavior of the hybrid structure was examined using the thermionic emission model [29]. According to this model, the junction under forward bias has the I–V relation as

$$I = I_{\mathrm{s}} \left[\exp\left(\frac{qV}{nk_{\mathrm{B}}T} \right) - 1 \right], \tag{1}$$

where I_{s} is the saturation current, q is the elementary charge, V is the applied forward voltage, n is the ideality factor, k_{B} is the Boltzmann constant, and T is the absolute temperature. The saturation current I_{s} is expressed as

$$I_s = AA^*T^2 \exp\left(\frac{-q\Phi_b}{k_B T}\right), \quad (2)$$

where A is the junction area, A^* is the effective Richardson constant with 32.4 A cm^{-2} K^{-2} for GaN ($m_e^* = 0.2m_0$) [30], and Φ_b is the barrier height at the GaN/polymer interface. The junction area in the present case is 5×10^{-2} cm^2. In order to find out the values of n and Φ_b of the hybrid structure, a graph of $\ln(I)$ against V was plotted.

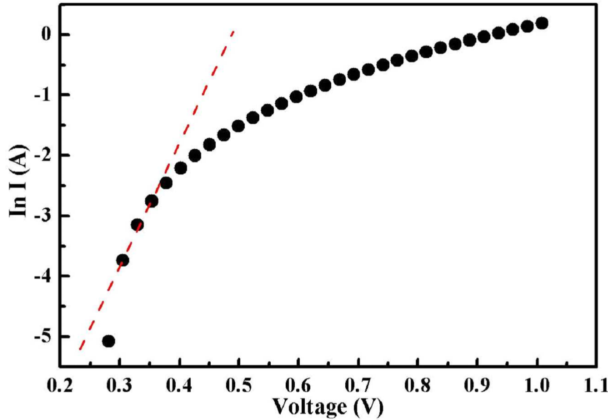

Fig. 6. Semilogarithmic plot of current ($\ln(I)$) and voltage (V) for the hybrid structure.

Figure 6 shows the semilogarithmic plot of current as a function of bias voltage. The slope and the intercept from the linear fit to the log plot yield the ideality factor, $n = 1.9$ ($n = 12.9$ for the PEDOT:PSS/GaN structure), the barrier height, $\Phi_b = 0.51$ eV ($\Phi_b = 0.40$ eV for the PEDOT:PSS/GaN structure). The ideality factor of a junction usually falls between 1 and 2. However, for the PEDOT:PSS/GaN structure, anomalous high ideality factor was obtained. The high ideality factors have been previously reported in a few *p–n* junctions [31] and heterojunctions [32]. The ideality factor of GaN based diode with multiple quantum wells is usually in the range between 5 to 7 [31, 33]. Furthermore, the fabrication of nanorod structure diode will damage the surface of devices easily which also contribute to high ideality factor (10 and 18 [34, 35]). However, the exact mechanism of this high ideality factor has not been fully understood. The ideality factor of the hybrid structure with PEDOT nanoparticle interface layer is dramatically decreased. The ideality factor of $n = 1.9$ indicates that the current transport mechanism is a combination of diffusion limited and space charge limited transport. This may be possible because the PEDOT nanoparticle embedded in the polymer layer contributes to hopping of carriers between the PEDOT:PSS chains. It is suggested that the PEDOT nanoparticle may be useful for one of the electron transport layers, which could be applied to hybrid structured devices.

4. Conclusion

A heavily Si-doped GaN/polymer hybrid structure with the PEDOT nanoparticle has been fabricated. The I–V characteristic of the hybrid structure shows diode-like behavior. The ideality factor of the hybrid structure was calculated by applying the thermionic emission model and was found to be 1.9 while that of the PEDOT:PSS/GaN structure exhibits anomalously high value. The ideality factor of the hybrid structure indicates that the current transport mechanism is a combination of diffusion limited and space charge limited transport induced by the PEDOT nanoparticle interface layer.

Acknowledgments

This research was supported by Basic Science Research Program through the National Research Foundation of Korea (NRF) funded by the Ministry of Education, Science and Technology (No. 2010-0016147).

References

[1] S. Nakamura, T. Mukai, M. Senoh, *Appl. Phys. Lett.* **64**, 28 (1994).

[2] M.A. Khan, J.N. Kuznia, A.R. Bhattarai, D.T. Olson, *Appl. Phys. Lett.* **62**, 1786 (1993).

[3] M.A. Khan, A.R. Bhattarai, J.N. Kuznia, D.T. Olson, *Appl. Phys. Lett.* **63**, 1214 (1993).

[4] M.A. Khan, J.N. Kuznia, D.T. Olson, J.N. Van Hone, M. Blasingame, L.F. Reitz, *Appl. Phys. Lett.* **60**, 2917 (1992).

[5] M.A. Khan, J.N. Kuznia, D.T. Olson, J.M. Van Hone, M. Blasingame, L.F. Reitz, *Appl. Phys. Lett.* **63**, 1 (1993).

[6] S. Nakamura, T. Mukai, M. Senoh, *Jpn. J. Appl. Phys.* **31**, 2883 (1992).

[7] G.-C. Yi, B.W. Wessels, *Appl. Phys. Lett.* **69**, 3028 (1996).

[8] J.W. Orton, C.T. Foxon, *Semicond. Sci. Technol.* **13**, 310 (1998).

[9] A. Usikov, O. Kovalenkov, V. Soukhoveev, V. Ivantsov, A. Syrkin, V. Dmitriev, A.Y. Nikiforov, S.G. Sundaresan, S.J. Jeliazkov, A.V. Davydov, *Phys. Status Solidi C* **6**, 1829 (2008).

[10] X.Q. Shen, M. Shimizu, H. Okumura, F.J. Xu, B. Shen, G.Y. Zhang, *J. Cryst. Growth* **311**, 2049 (2009).

[11] J.H. Yang, S.M. Kang, D.V. Dinh, D.H. Yoon, *Thin Solid Films* **517**, 5057 (2009).

[12] X.W. Sun, J.Z. Huang, J.X. Wang, Z. Xu, *Nano Lett.* **8**, 1219 (2008).

[13] M. Willander, O. Nur, N. Bano, K. Sultana, *New J. Phys.* **11**, 125020 (2009).

[14] M. Nakano, A. Tsukazaki, R.Y. Gunji, K. Ueno, A. Ohtomo, T. Fukumura, *Appl. Phys. Lett.* **88**, 142113 (2007).

[15] D.M. Welsh, A. Kumar, E.W. Meijer, J.R. Reynolds, *Adv. Mater.* **11**, 1379 (1999).

[16] A. Laforgue, P. Simon, J.F. Fauvarque, M. Mastragostino, F. Soavi, J.F. Arrau, E. Rossi, S. Saguatti, *J. Electrochem. Soc.* **150**, A645 (2003).

[17] D.M. Leeuw, P.A. Kraakman, P.E.G. Bongaerts, C.M.J. Mutsaers, D.B.M. Klaassen, *Synth. Met.* **66**, 263 (1994).

[18] X. Gong, D. Moses, A.J. Heeger, S. Liu, A.K.Y. Jen, *Appl. Phys. Lett.* **83**, 193 (2003).

[19] J. Inoue, K. Yamagishi, M. Yamashita, *J. Cryst. Growth* **298**, 782 (2007).

[20] H. Yoon, M. Chang, J. Jang, *Adv. Funct. Mater.* **17**, 431 (2007).

[21] L. Groenendal, G. Zotti, P.-H. Aubert, S.M. Waybright, J.R. Reynolds, *Adv. Mater.* **15**, 855 (2003).

[22] T. Imae, C. Li, *Macromolecules* **37**, 2411 (2004).

[23] K. Müller, M. Klapper, K. Müllen, *Macromol. Rapid Commun.* **27**, 586 (2006).

[24] X. Zhang, J.-S. Lee, G.S. Lee, D.-K. Cha, M.J. Kim, D.J. Yang, S.K. Manohar, *Macromolecules* **39**, 470 (2006).

[25] M.G. Han, S.P. Armes, *Langmuir* **19**, 4523 (2003).

[26] X. Sun, M. Hanger, *Macromolecules* **40**, 8537 (2007).

[27] J.-C. Song, S.-H. Lee, I.-H. Lee, K.-W. Seol, S. Kannappan, C.-R. Lee, *J. Cryst. Growth* **308**, 321 (2007).

[28] K. Kim, J. Choi, M. Jung, D.H. Woo, *Jpn. J. Appl. Phys.* **47**, 6354 (2008).

[29] L.S. Chuah, Z. Hassan, H.A. Hassan, N.M. Ahmed, *J. Alloys Comp.* **481**, L15 (2009).

[30] Z.N. Dmitri, L.-W. Zuzanna, G. Yan, H. Evelyn, *J. Electron. Mater.* **35**, 1543 (2006).

[31] J.M. Shah, Y.L. Li, T. Gessmann, E.F. Schubert, *J. Appl. Phys.* **94**, 2627 (2003).

[32] M. Campos, G. Casalbore-Miceli, N. Camaioni, *J. Phys. D, Appl. Phys.* **28**, 2123 (1995).

[33] K. Mayes, A. Yasan, R. McClintock, D. Shiell, S.R. Darvish, P. Kung, M. Razeghi, *Appl. Phys. Lett.* **84**, 1046 (2004).

[34] P. Deb, H. Kim, Y. Qin, R. Lahiji, M. Oliver, R. Reifenberger, T. Sands, *Nano Lett.* **6**, 2893 (2006).

[35] A. Motayed, A.V. Davydov, M.D. Vaudin, I. Levin, J. Melngailis, S.N. Mohammad, *J. Appl. Phys.* **100**, 024306 (2006).